Human cortical neural stem cells generate regional organizer states *in vitro* before committing to excitatory neuronal fates

Nicola Micali[1,2], Suel-Kee Kim[1], Marcelo Diaz-Bustamante[1], Genevieve Stein-O'Brien[1,3], Seungmae Seo[1], Joo-Heon Shin[1], Brian G. Rash[2], Shaojie Ma[4], Nicolas A. Olivares[1], Jon Arellano[2], Kristen R. Maynard[1], Elana J. Fertig[5,6,7], Alan J. Cross[8], Roland Burli[8], Nicholas J. Brandon[8], Daniel R. Weinberger[1,3,9,10,11], Joshua G. Chenoweth[1], Daniel J. Hoeppner[1,14], Nenad Sestan[2,4,12], Pasko Rakic[2,12], Carlo Colantuoni[1,9,11,13], Ronald D. McKay[1*]

[1] Lieber Institute for Brain Development, 855 North Wolfe, Baltimore, MD 21205, USA

[2] Department of Neuroscience, Yale School of Medicine, New Haven, CT 06520, USA

[3] McKusick-Nathans Institute of Genetic Medicine, Johns Hopkins School of Medicine, Baltimore, MD 21205, USA

[4] Departments of Comparartive Medicine, of Genetics, and of Psychiatry, Yale School of Medicine, New Haven, CT 06520, USA

[5] Department of Oncology, Sidney Kimmel Comprehensive Cancer Center, Johns Hopkins School of Medicine, Baltimore, MD 21205, USA

[6] Department of Biomedical Enginneering, Johns Hopkins School of Medicine, Baltimore, MD 21205, USA

[7] Department of Applied Mathematics and Statistics, Johns Hopkins University, Baltimore, MD 21218, USA

[8] AstraZeneca Neuroscience, IMED Biotech Unit, R&D Boston, MA 024515, USA

[9] Department of Neurology, Johns Hopkins School of Medicine, Baltimore, MD 21205, USA

[10] Department of Psychiatry, Johns Hopkins School of Medicine, Baltimore, MD 21205, USA

[11] Department of Neuroscience, Johns Hopkins School of Medicine, Baltimore, MD 21205, USA

[12] Kavli Institute for Neuroscience, Yale School of Medicine, New Haven, CT 06520, USA

[13] Institute for Genome Sciences, University of Maryland School of Medicine, Baltimore, MD 21201, USA

[14] Present affiliation: Astellas Research Institute of America, 3565 General Atomics Ct., Ste. 200 San Diego, CA 92121, USA

[*] Corresponding author and lead contact ronald.mckay@libd.org

Keywords: Neural stem cells, corticogenesis, FGF2, BMP, transcriptional dynamics, human neurogenesis, cortical evolution, EGFR, neuronal differentiation, patterning of the cortex

SUMMARY

Better understanding of the mechanisms underlying the developmental progression of neural stem cells (NSCs) in the cerebral cortex is important for modeling neurogenesis and defining the pathogenesis of neuropsychiatric disorders. Here we used RNA-sequencing, cell imaging and lineage tracing of mouse, macaque and human neurogenesis, along with single-cell RNA-sequencing and immuno-labeling to explore how cortical glutamatergic excitatory neurons are generated *in vitro* and *in vivo*. This analysis revealed that conserved signaling mechanisms regulate glutamatergic neurogenesis among the three species. We then show that as human telencephalic NSCs develop *in vitro,* they first generate the organizer states that spatially pattern the cortex before progressing to excitatory neuronal fates. This developmental progression of human NSCs *in vitro* opens to systematic analysis key aspects of human-specific area patterning during cortical neurogenesis.

INTRODUCTION

Defining how cell types emerge in the forebrain is a central topic in the quest to understand the origins of the normal and pathological function of the cerebral cortex (Geschwind and Rakic, 2013; Kwan et al., 2012b; Lein et al., 2017; Nowakowski et al., 2017; Sandberg et al., 2016; Wamsley and Fishell, 2017). The excitatory and inhibitory neurons of the cortex emerge in two different rostral neuroepithelial zones, the dorsal and ventral telencephalon (Kwan et al., 2012b; Sandberg et al., 2016; Wonders and Anderson, 2006). Evidence of genetic risk for neuropsychiatric disorders has been found in the patterns of genes expressed in the midfetal neurogenic cortex (Gulsuner et al., 2013; Parikshak et al., 2013; State and Sestan, 2012; Willsey et al., 2013; Xu et al., 2014). Moreover, risk associated genes have been identified in the *in vitro* functional phenotypes of NSCs derived from patient-specific induced pluripotent stem cells (iPSCs) (Brennand et al., 2015; Consortium, 2017; Fujimori et al., 2018; Lang et al., 2018; Madison et al., 2015; Marchetto et al., 2016; Mariani et al., 2015). Thus, understanding the signaling specifying cortical NSCs *in vitro* is required to define pathogenic mechanisms and develop new therapies for brain disorders.

The neocortex in mammals, including rodents and humans, is the product of fate transitions of radial glial cells (RGCs) sequentially generating in the proliferative zones post-mitotic neurons, that migrate to distinct overlying cortical layers where they carry out different circuit functions (Angevine and Sidman, 1961; Rakic, 1974, 1988). This *in vivo* evidence points to the importance of accurately defining how cortical neuronal fate commitment is controlled *in vitro*. It is well established that in cell culture, the growth factor status of the medium regulates the transition from proliferating NSCs to differentiated progeny (Cattaneo and McKay, 1990; Johe et al., 1996; Ravin et al., 2008). Widely studied intracellular regulators of NSC growth include the Ras-extracellular signal-regulated kinase (RAS-ERK) and the phosphatidylinositol 3 kinase-protein kinase B-mammalian target of rapamycin (PI3K-AKT-mTOR) signaling pathways, that also play a major role in brain cancer, as well as neurodevelopmental diseases (Crawley et al., 2016; Ernst, 2016; Mendoza et al., 2011). FGF2, insulin and other extracellular ligands, acting through the

MAPK/ERK and PI3K/AKT pathways on the expression of cell cycle regulators, control the critical transition when cortical NSCs initiate neurogenesis, both in brain development and cell culture (Adepoju et al., 2014; Androutsellis-Theotokis et al., 2006; Lehtinen et al., 2011; Qi et al., 2017; Rash et al., 2011; Vaccarino et al., 1999). The withdrawal of the NSC growth factor FGF2 has been widely used to stimulate neurogenesis *in vitro* (Cattaneo and McKay, 1990; Johe et al., 1996), and lineage analysis under this condition directly demonstrates rapid commitment of multi-potential NSCs to neuronal and glial fates (Ravin et al., 2008). However, we lack direct evidence showing that cortical neurons are specified when they become post-mitotic *in vitro*. Here, we show that modulating FGF2-MAPK signaling controls the timing of cell cycle exit and the developmental progression of NSCs to distinct differentiation trajectories. This analysis demonstrated that specification of glutamatergic excitatory cortical neurons is dependent on conserved signaling mechanisms operating as proliferating mouse and human NSCs become post-mitotic.

In the developing mammalian telencephalon, before neurons are specified, organizer centers emerge to pattern different cortical domains (Geschwind and Rakic, 2013; Grove and Fukuchi-Shimogori, 2003; O'Leary et al., 2007; Sur and Rubenstein, 2005). Recent reports of species-specific differences in corticogenesis are often focused on relatively late neurogenic stages where there is an enhanced genesis of superficial neurons in the primate outer subventricular zone (oSVZ) (Namba and Huttner, 2017; Nowakowski et al., 2016; Zhu et al., 2018). However, evolutionary expansion of the cerebral primordium is evident from the earliest stages, even before the onset of corticogenesis, and is already prominent when RGCs produce the first glutamatergic neurons (Bystron et al., 2008; Geschwind and Rakic, 2013). Thus, there is a clear interest in defining the early signaling mechanisms that specify neurogenesis in different mammalian species, including humans. Building on previous work (Edri et al., 2015), we now show that NSCs derived *in vitro* from human PSCs self-organize to sequentially occupy different developmental stages. Early passages of human NSCs were highly enriched in cells expressing genes characteristic of the cortical hem, an organizer zone that patterns the neocortex (Caronia-

Brown et al., 2014). At later passages the neural rosettes representing excitatory cortical neuronal precursors were generated at high frequency. These data indicate that cortical patterning mechanisms and neuronal fate commitment are coordinated features that progress under precise controls in NSCs *in vitro*, providing access into the early mechanisms specifying the cellular architecture of the human cerebral cortex.

RESULTS

Early FGF2 signaling in mouse NSCs regulates cortical neurogenesis *in vitro*

Rodent cortical NSCs proliferate maximally in the presence of 10 ng/ml FGF2 and abruptly differentiate when this growth factor is withdrawn, *in vitro* (Adepoju et al., 2014; Cattaneo and McKay, 1990; Ravin et al., 2008). Here, primary NSC cultures were derived from mouse dorsal telencephalon at the beginning of neurogenesis, embryonic day 11.5 (E11.5), and expanded. NSCs were exposed to a range of FGF2 doses (0.1, 1, or 10 ng/ml) for 48 hours after passage, and their later differentiation monitored (Figure 1A). The cultures exposed to lower (0.1 or 1.0 ng/ml) rather than the higher (10 ng/ml) dose of FGF2 generated more neurons, assessed at day *in vitro* (DIV) 15 (Figure 1B). Molecular differences between cortical glutamatergic excitatory projection (pyramidal) neurons have been used to define the appearance of distinct neuron subtypes found in different layers (Kwan et al., 2012b; Molyneaux et al., 2007; Shen et al., 2006) (Figure S1A). The highest FGF2 dose (10 ng/ml) generated lower numbers of neuron types at all times, as defined by immunostaining for TLE4 and CUX1, well established markers of deep and upper layer projection neurons (Figure 1C). These results show that the FGF2 signaling status of NSCs exiting the cell cycle regulates the generation of glutamatergic neurons.

Next, we examined the distribution of synapses and electrophysiological activity after two weeks of neurogenesis (Figure 1D and S1B). The density of puncta expressing the synaptic marker Synapsin 1 (SYN1) was significantly higher in neurons derived from the low FGF2 conditions (Figure S1B). The synaptic proteins Homer1 (HOM1) and PSD95, and the density of puncta co-localizing these pre- and post-synaptic markers were higher in neurons derived from treatment

with 1 ng/ml FGF2 (Figure S1B), which also showed the highest frequency of spontaneous excitatory postsynaptic currents (EPSC) (Figure 1D). Similar results were observed later at DIV 22 (Figure S1C). These data confirm that FGF2 signaling during the initial *in vitro* differentiation of NSCs regulates the number, type and activity of the derived cortical neurons many days later.

Waves of transcriptional dynamics during mouse *in vitro* neurogenesis

To gain insight into the transcriptional dynamics responsible for these changes in neuronal differentiation, mouse cortical NSCs were exposed to varying doses of FGF2 and total RNA was collected for deep sequencing (RNA-seq), from 6 hours to 12 days of differentiation (Figure 1A). Principal component analysis (PCA) defined progressive differentiation in PC1 (Figure S2A) indicating NSCs exposed to lower FGF2 concentrations moved more rapidly through this major transition in gene expression.

Gene expression data can be visualized or "projected" into a low-dimensional space defined by another data set. This allows the exploration of transcriptional modules of the first data set as they change in the new data space. To relate the dynamics of mouse NSCs *in vitro* to *in vivo* cortical development, we projected expression data from the developing human (Jaffe et al., 2018) and macaque neocortex (Bakken et al., 2016) into the transcriptional space defined by the individual gene weights from PC1, using ProjectR (Figure S2Bi and ii; see Methods for details and www.biorxiv.org/content/early/2018/08/20/395004.1). These projections demonstrate that the dimension of greatest change in the *in vitro* mouse PC1 data parallels *in vivo* development, and encourage further analysis of the conserved transcriptional dynamics between the *in vitro* neurogenesis and the *in vivo* development of the human and macaque cerebral cortex.

To gain a higher resolution view of transcriptional dynamics during neural differentiation, we employed the genome-wide CoGAPS (GWCoGAPS) non-negative matrix factorization (NMF) method, that assigns weights for the contribution of every gene to a set number of patterns, to represent dominant changes in gene expression across all the *in vitro* samples (Fertig et al.,

2014; Stein-O'Brien et al., 2017). GWCoGAPS analysis, identifying 11 patterns (p1-11; Figure 1E and S2C and D), defined sequential waves of transcriptional extinction and induction as NSCs differentiated. Hierarchical clustering ordered these patterns into three groups associated with: (1) NSC expansion (p5 and p6); (2) initiation of neural differentiation (p1, p11, p7, p9 and p10); and (3) further maturation (p9, p10, p4 and p8) (Figure S2C and D). The early patterns (p5 and p6) were maintained in high FGF2 dose and enriched in cell cycle regulator genes, defined by GO analysis (Figure 1E). As differentiation proceeds, the initial FGF2 condition controlled sequential waves of gene expression in the first 6 days of differentiation (patterns p1, p11, p7 and p9) (Figure 1E and S2D). For later steps of differentiation, GO analysis defined distinct end points for low and high FGF2 conditions that reflect either terminal neuro- (p8; low FGF2) or glio- (p4; high FGF2) genesis (Figure 1E).

These data show that NSCs passaged into low FGF2 doses abruptly down regulated cell cycle genes and traversed later steps of neuron differentiation more rapidly (Figure S3A and B). Consistent with this transcriptional analysis and our previous work (Adepoju et al., 2014), phosphorylation of MAPK/ERK and expression of Cyclin D1 were sensitive to FGF2 dose (Figure S3C), and synaptic maturation genes including CaMKIIα increased when NSCs abruptly left the cell cycle in low FGF2 (Figure S3D). This analysis defines dynamic waves of transcription, initiated by variation in FGF2 signaling as NSCs exit the cell cycle, implementing distinct differentiation trajectories biased towards either cortical neurons or glia.

Endogenous early BMP function is required for mouse cortical neurogenesis

To more precisely define the events initiating the differentiation of dorsal telencephalic neurons *in vitro*, we focused on BMP signaling that is known to oppose FGFs in patterning the telencephalon *in vivo* and regulating NSC differentiation *in vitro* (Lehtinen et al., 2011; Lillien and Raphael, 2000; Mabie et al., 1999; Tiberi et al., 2012). When the expression patterns of BMP signaling genes were analyzed during *in vitro* neurogenesis, distinct waves of expression correlated with particular BMP ligands and BMP responsive gene sets were observed (Figure 1E patterns p7, 2A-D and

S4A). Nuclear phosphorylated SMAD1/5 (pSMAD1/5) signal showed transient and rapid induction of endogenous BMP signaling in low FGF2 dose (Figure 2E), alongside BMP4 and Noggin mRNA expression (Figure 2B and D).

To determine if this early BMP signaling had a significant effect on later steps of neuronal maturation, BMP type I receptors were blocked with the inhibitor LDN193189, at 12 hours after plating and prior to BMP4 transcription. The early inhibition of BMP signaling blocked both pSMAD1/5 induction at DIV 2 and the subsequent synaptic maturation seen at DIV 15 at low FGF2 doses (Figure 2F and 2G). NOTCH and WNT signaling genes also showed temporal dynamics across neurogenesis (Figure S4B), suggesting that these signaling pathways also orchestrate these transitions. The data shown here indicate that FGF2 regulated an endogenous BMP signaling wave during the transition from proliferation to differentiation that was necessary for cortical neurogenesis and synaptic maturation.

Two mouse cortical NSC subtypes show selective FGF2 induced BMP signaling activation and distinct fate bias

We previously demonstrated that rodent cortical NSCs consist of a heterogeneous and dynamic population with varying lineage potential (Ravin et al., 2008). To further explore NSC diversity during cortical neurogenesis *in vitro*, we interrogated the surface expression of the tyrosine kinase receptors PDGFRα and EGFR which mark subsets of NSCs *in vitro* and *in vivo* (Jackson et al., 2006; Lillien and Raphael, 2000; Sun et al., 2005). Remarkably, the proportion of PDGFRα$_{high}$ and EGFR$_{high}$ cells was regulated by FGF2 dose in the first 2 days *in vitro* and the expression of the receptors was mutually exclusive and decresed at DIV 6, indicating that FGF2 treatment induces a transient wave of EGFR positive cells from a PDGFR positive state (Figure 3A and S5A).

Time-lapse recording and lineage analysis showed that FGF2 signaling controlled the cell cycle duration of EGFR$_{high}$ cells (Figure S5B). EGFR$_{high}$ cells showed higher levels of phosphorylated

FGF receptor (pFGFR) and pERK across all FGF2 doses (Figure S5C), but no differences in FGFR2, FGFR1 and FGFR3 expression were seen (Figure S5C, not shown). HES1 and PAX6 expression were higher in $EGFR_{high}$ cells, while SOX2 expression level was higher in $PDGFR\alpha_{high}$ cells (Figure S5D). Consistent with the induction of endogenous BMP signaling as cortical neurons differentiate, phospho-SMAD1/5 and BMPR1A levels were higher in $EGFR_{high}$ cells (Figure 3B). These results show that the FGF2 status at cell passage initiates BMP signaling in a transient $EGFR_{high}$ differentiating state.

To assess the fate bias of these different NSC subtypes, we performed time-lapse recording to create lineage dendrograms linking $EGFR_{high}$ or $PDGFR\alpha_{high}$ founder cells at DIV 1 to the corresponding neurons, oligodendrocytes and astrocytes, identified at DIV 6 by expression of TuJ1, O4 or GFAP (Figure S6Ai; Video S1-3). $PDGFR\alpha_{high}$ progenitors generated similar proportions of oligodendrocytes and neurons in low FGF2 conditions, and predominantly gave oligodendrocytes at the higher FGF2 dose. $EGFR_{high}$ cells were tripotent, both in 1 and 10 ng/ml FGF2. Importantly, the timing of lineage specification events (see methods and (Ravin et al., 2008)) showed that increasing FGF2 doses delays cell cycle exit and shifts fate specification to later generations (Figure 3C and S6Aii).

To lineage trace neurons at more mature stages of differentiation (DIV 15), we employed adeno-associated viruses (AAV) encoding green fluorescent protein (GFP) with preferential tropism for cells expressing either PDGFRα (AAV5) or EGFR (AAV6) (Di Pasquale et al., 2003; Jackson et al., 2006; Weller et al., 2010) (Figure S6B and C). AAV6-infected cells preferentially generated $CUX1^+$, $FOXP2^+$, or $TLE4^+$ glutamatergic neurons, while AAV5-infected cells generated more GAD65 expressing putative GABAergic neurons with less complex neuronal morphologies (Figure 3D and S6D). These results indicate that mouse telencephalic NSCs exposed to low FGF2 generate an $EGFR_{high}$ BMP responsive cell that specifically differentiates to neurons with cortical glutamatergic fates.

Cortical neuron differentiation bias varies with the passage of human NSCs

Neuroepithelial fates with dorsal telencephalic features can be generated from human pluripotent stem cells *in vitro* (Edri et al., 2015; Mariani et al., 2012; Shi et al., 2012), however the specific details of neuronal commitment are not known. To explore the mechanisms of human cortical neurogenesis, we differentiated the embryonic stem cell (ESC) line H9 to telencephalic NSCs that were then serially passaged (Figure S7A) (Chambers et al., 2009; Edri et al., 2015). hNSCs grown in 20 ng/ml FGF2 were analyzed for the expression of the fate regulators SOX2, HES1, HES5, OTX2, PAX6 and SOX21 through passages 1 to 5 (PS1-5) (Figure S7B and C). The results show the spontaneous emergence and decline of the rosette-forming neurogenic state, providing a rich substrate to define human neurogenic mechanisms.

To explore the neurogenic potential of these dynamic NSC states, RNA-seq was performed 6 days after hNSCs were exposed to varying concentrations of FGF2 at the terminal passage, from passages 1 to 8 (PS1-PS8; see Methods) (Figure 4A and S7A). PC1 revealed transcriptional progression across passages that was independent of FGF2 treatment (Figure S7Di). Projection analysis using ProjectR indicated parallels between the transcriptional dynamics identified by PC1 *in vitro* and the developing human (Jaffe et al., 2018) and macaque (Bakken et al., 2016) cortices (Figure S7Dii and iii). To characterize these transcriptional dynamics at a more granular level, we explored a set of 24 patterns (p1-24) defined by the GWCoGAPS NMF algorithm in the hNSC RNA-seq dataset that describe gene expression change upon FGF2 modulation at every passage (Figure S8A). Patterns p5, p6 and p22 showed transcriptional differences across FGF2 dose specific to PS4, when neural rosettes were most abundant (Figure 4Bi and S8A, S7B and C). Projection of macaque data (Bakken et al., 2016) into these patterns shows that p5 specifically identifies a gene signature that is highly expressed in the forming cortical plate (CP) over the germinal domains SVZ and VZ throughout this neurogenic period (Figure 4Bii).

To more precisely relate the *in vitro* transcriptional dynamics to discrete cell types of the developing primate neocortex, we performed single-cell mRNA sequencing (scRNA-seq) in E78

rhesus macaque embryonic dorso-lateral prefrontal cortex (DLPFC) using 10x Genomic platform. Data from 4376 single cells passed quality control meaures and were included in the present study. Using unsupervised clustering, we identified 6 distinct clusters representing excitatory neurons, NSCs, oligodendrocytes, microglia, astrocytes and endothelial cells (Figure S9A and B). Projection of these scRNA-seq data into gene weights from *in vitro* hNSC GWCoGAPS patterns confirms that p5 correlated with post-mitotic neurons *in vivo* (Figure 4Biii). Of note, p22, induced by high FGF2 treatment, was not associated with a neurogenic signature in either projection. These results indicate that the *in vitro* appearance of new-born cortical neurons was favored specifically at PS4 by acute reduction of FGF2 and, importantly, suggests that parallel gene expression dynamics occurred *in vitro* and in the neurogenic primate neocortex.

Immunofluorescence was used to further explore the differentiation of post-mitotic neurons from PS4 hNSCs. The data show that low FGF2 favored a switch from proliferating (EDU^+) hNSCs, $SOX2^+$ and $PAX6^+$, to $PAX6^-$, $SOX2^-$, $TuJ1^+$, $EGFR_{high}$, Doublecortin $(DCX)^+$-expressing post-mitotic (EDU^-) early-born neurons (Figure 4C and S7B, S8Biii-v and C). Elevated pSMAD1/5 immunoreactivity showed that differentiation in low FGF2 was associated with a burst of endogenous BMP signaling, which occurs specifically at the neurogenic passage PS4 (Figure 4C and S8B).

When PS4 hNSCs were differentiated for a more extended period, more neurons expressing markers of cortical layers (TBR1, FOXP2 or SATB2) and showing synaptic activity and action potentials were derived from hNSCs treated with low doses of FGF2 (Figure 4D and E, and S8D). These results suggest that neurons with cortical glutamatergic features were specified by a conserved mechanism in human and mouse NSCs and, importantly, that hNSCs differ with the passage in the generation of these pertinent neuronal intermediates (Figure S8Bi-iv).

EGFR-BMP signaling interaction defines an early neuronal transition state of RGCs in developing primate cortex

Next, we investigated in rhesus macaque whether the developmental progression of NSC states *in vivo* resembled that seen *in vitro*. In the prenatal macaque dorsal parietal cortex, $EGFR_{high}/PAX6^{+}$ RGCs, detected by immuno-histochemistry in the VZ/iSVZ at E70, but not at the beginning of corticogenesis at E55 (not shown), identified neural progenitors and early committed neurons (Hansen et al., 2010; Mo and Zecevic, 2008) that delaminated spanning the oSVZ (Figure 4Fi, ii, and S9Ci). The induction of nuclear pSMAD1/5 in the $EGFR_{high}$ RGCs indicates BMP signaling response in the VZ/iSVZ, which is an early step in neuronal differentiation (Lehtinen et al., 2011; Li et al., 1998; Saxena et al., 2018) (Figure 4Fii and iii, S9Cii). Moreover, we found $EGFR_{high}$ RGCs expressing the neurogenic transcription factors EOMES/TBR2 and NEUROD1 in iSVZ, confirming neuron fate commitment of these cells (Figure 4Fiii and iv, S9Cii and iii) (Arnold et al., 2008; Englund et al., 2005; Pollen et al., 2015). Interestingly, EGFR staining was not detected in cells expressing late neuronal markers, such as $TBR1^{+}$ cells in the cortical plate, and no $EGFR_{high}/NEUROD1^{+}$ cells were found in the intermediate zone or CP (Figure 4Fv and S9Cii and iii).

The dynamics of expression of genes as human telencephalic neural stem cells become post-mitotic was explored in a single cell RNA-seq data (Nowakowski et al., 2017). The overall structure of cell types in these data was established by tSNE analysis demonstrating the clear distinction between the cascade of differentiating neurons seen in the ventral and dorsal telencephalon (Figure S9D). Proliferative and non-proliferative neuronal intermediate precursors cells (IPCs) in the dorsal telencephalic trajectory were identified (Figure 4G). Proliferating $TBR2^{+}/SOX2^{+}$ neuronal IPCs could also express EGFR and respond to endogenous BMPs, while more mature non-cycling $TBR2^{+}$ cells were $SOX2^{-}/EGFR^{-}$ and negative for any BMP signaling related gene (Figure 4G and S9D). These data confirm that dynamic EGFR expression is an early and transient step in the generation of neurons from RGCs, in primate cortical neurogenesis. Together, these results are consistent with the hypothesis that in the mid-neurogenic phase of monkey and human cortex, an $EGFR_{high}$ cell population employing BMP signaling is an early transition state from proliferative RGCs to committed glutamergic cortical neurons.

Early passage human NSC states show cortical organizer identities

These events specifying cortical excitatory neuronal fates occur *in vivo* in a spatially constrained neuro-epithelial sheet patterned by morphogenetic signals from adjacent organizer domains. To understand how cortical neuronal precursors at PS4 were generated, we focused on the GWCoGAPS patterns from the *in vitro* hNSC data showing the highest gene expression in PS2 and PS3 (Figure 5Ai and S10Ai). Patterns p2, p11, p4 and p19 but not p8 were dependent on the initial FGF2 status of the cells. These transcriptional dynamics at PS2 and PS3 suggest these early stages of human NSCs also undergo a differentiation response regulated by FGF-MAPK signaling and we explore their meaning further.

Projection of the developing macaque cortex gene expression data (Bakken et al., 2016) into these patterns showed that p8 and the low FGF2 patterns p11 and p2 were most highly represented in the cortical hem domain (Figure 5Aii; (Bakken et al., 2016)). Importantly, neither the high FGF2 patterns p4 and p19, nor the later patterns p5 and p22 (described above), showed enrichment in genes of the cortical hem domain (Figure S10Aii and 4Bii). This analysis indicates that the low FGF2 conditions at early passages p2 and p3 induced elements of the hem transcriptional signature. The cortical hem zone is a source of BMP and WNT morphogens that pattern the dorsal and caudal domain of the telencephalon (Caronia-Brown et al., 2014; Grove et al., 1998). In order to monitor the emergence of this cellular organizer identity across the passages, we used the gene expression data from the developing macaque cortex (Bakken et al., 2016) to generate a list of hem-specific genes (see Methods; Figure 5B). Passages 2 and 3 were enriched in these genes including LMX1A, WNT8B, WNT3A, BMP2/4/6/7, RSPO1/2/3 and BAMBI indicating coordinated expression at early passages *in vitro* of many hem regulators (Figure 5B and S10B).

Consistent with the known function of LMX1A in mouse organizers including the cortical hem (Chizhikov et al., 2010), expression of this transcription factor (TF) was highest at PS2 in low

FGF2 and subsequently decreased (Figure 5Ci and iv). In contrast, the TFs FOXG1 and LHX2, which are required in the mouse to form the medial pallium and lateral cortex and to repress the formation of the cortical hem (Bulchand et al., 2001; Hanashima et al., 2007; Mangale et al., 2008; Molyneaux et al., 2007; Monuki et al., 2001), appeared at later passages (Figure 5Ci, ii, iv, v). At passage 3, the majority of cells expressed LMX1A or LHX2, suggesting co-emergence of the caudal hem organizer and the precursor cells of the cortical field (Figure 5Civ). The expression patterns of genes such as FGF8, TTR, and SFRP2 at these early passages suggest that the anterior patterning center, the choroid plexus, and the antihem were also represented (Figure S10C). The progressive appearance at PS3 of $OTX2^{+}$, a transcriptional regulator of the choroid plexus and cortical hem (Sakaguchi et al., 2015), $FOXG1^{+}$ cells and then of $OTX2^{-}$, $FOXG1^{-}$, $EGFR_{high}$ cells at PS4 (Figure 5Cii, iii and v) confirms these hNSCs progress from a hem- to a cortex-like identity (Figure 5C and D). This coordinated change indicates that cortical patterning and neuronal specification mechanisms are efficiently executed across early passages of human neural precursors *in vitro*.

DISCUSSION

Controlling the early cellular events during neurogenesis is essential to model brain development. In the present study, we first definitively show that proliferating mouse and human NSCs commit to excitatory cortical neuronal fates as they become post-mitotic. Prior to the phase when excitatory neurons were most efficiently generated, human NSCs transitioned through organizer and pallial precursor states recapitulating early steps in the patterning and neurogenesis of the cerebral cortex. The mechanisms of neuronal commitment in primary mouse and human cortical NSCs expanded *in vitro* were analyzed using a combination of cell lineage, signaling and transcriptomic tools. These results defined molecular and cellular dynamics at the time NSCs become post-mitotic and commit to cortical excitatory neuronal fates. Remarkably, FGF2 signaling generated asymmetry within NSC progenitors *in vitro*, instructing populations characterized by high levels of EGFR expression to take on cortical neuronal fates. When mouse and human NSCs were passaged in low doses of FGF2, $EGFR_{high}$ cells responsive to

endogenous BMP signaling were generated as cortical glutamatergic neurons first differentiated. At higher FGF2 concentrations we observed delayed BMP activity and additional cycles of proliferation prior to cell cycle exit, leading preferentially to glial (oligodendrocytic and astrocytic) and neuronal fates that did not include canonical excitatory neurons. The results here support a model where the commitment of NSCs to cortical neuronal fates is determined by modular cell state progressions initiated by the precise signaling conditions active during cell cycle exit.

Extending previous work identifying EGFR expressing cells as astro-glial precursors of the late SVZ in rodents (Burrows et al., 1997; Lillien and Raphael, 2000; Sun et al., 2005) and monkey (Rash BG et al, *PNAS* 2019, in press), our work defines a transient population of proliferative neurogenic $EGFR_{high}$ RGCs in the VZ/iSVZ undergoing acute neuronal commitment during monkey and human cortical development. *In vitro* and *in vivo* data suggest that EGFR-BMP signaling interaction defines mouse, monkey and human RGCs committed to cortical neurogenic fates. Our report that *in vitro* signaling and transcriptional dynamics parallel *in vivo* systems encourages further analysis of the mechanisms of cortical excitatory neuronal commitment *in vitro*.

From the first generation of neurons from pluripotent sources *in vitro* (Kim et al., 2002; Okabe et al., 1996) to the many recent studies of the transcriptomic and epigenetic landscapes of the developing cerebral cortex (de la Torre-Ubieta et al., 2018; Nowakowski et al., 2017; Zhu et al., 2018), it is becoming clear that NSC differentiation requires precise temporal and spatial regulation of cellular identities. Here, after demonstrating the most efficient generation of excitatory neurons occurred at a specific early passage, we explored the origins of this neurogenic state focusing on the regional patterning mechanisms, known *in vivo* to intrinsically coordinate the overall cortical structure prior to the inputs induced by the thalamic afferents (Armentano et al., 2007; Bishop et al., 2000; Cholfin and Rubenstein, 2007; Miyashita-Lin et al., 1999; Nakagawa et al., 1999; Shimogori and Grove, 2005). The two-dimensional architecture of the cortical field emerges from signaling interactions between the developing dorsal

telencephalon and spatially constrained specialized organizer cells (Fukuchi-Shimogori and Grove, 2001; Rash and Grove, 2006). We demonstrate the precise appearance of organizer and cortical precursor domains *in vitro*, providing an unprecedented opportunity to define how morphogenetic spatial patterning is co-ordinated with the specification of excitatory neurons in different regions of the human dorsal telencephalon.

The early developmental mechanisms operating in the telencephalon are proximal to genetic risk for neurodevelopmental disorders including autism spectrum disorder (ASD) (Marchetto et al., 2016; Mariani et al., 2015), bipolar disorder (Madison et al., 2015), fragile X syndrome (Kwan et al., 2012a), Huntington's disease (Consortium, 2017) and brain cancers (Crawley et al., 2016; Ernst, 2016). In the context of an unprecedented transcriptomic and epigenetic mapping of the human central nervous system (Amiri et al., 2018; de la Torre-Ubieta et al., 2018; Li et al., 2018; Wang et al., 2018; Zhu et al., 2018), progress continues in defining disease relevant *in vitro* phenotypes as a central tool in the development of novel therapeutic interventions (Fujimori et al., 2018; Hubler et al., 2018; Lang et al., 2018). To achieve accurate models of risk for neuro-psychiatric disease, it will be valuable to assess how patient-specific iPSCs vary as they progress through the non-linear developmental transitions described here. Our work supports the more precise definition of risk mechanisms by focusing attention on specific cell state transitions which involve TFs including FOXG1, a regulator of neural fate choices in the forebrain and involved in ASD (Mariani et al., 2015), or EOMES/TBR2 and FGFR2, whose human specific/gained enhancers (HGEs) are known to regulate early cortical fate choices, and their action in the cortical germinal zone, is implicated in neuro-developmental disorders including schizophrenia (de la Torre-Ubieta et al., 2018). Integration of the cell state transitions defined in this study with the emerging transcriptomic, epigenetic and functional maps of human forebrain, will yield new insight into the origin of developmental risk for neuro-psychiatric disorders.

AUTHOR CONTRIBUTIONS

N.M. and R.D.M. conceived the study. N.M. and SK.K. performed mouse and human stem cell culture and differentiation. N.M. performed all samples collection, adenovirus infections, data collection. N.M., N.A.O., M.D.B. performed rat astrocytes culture. M.D.B. performed electrophysiology. JH.S. generated RNA-seq data. G.SO., E.J.F., C.C. processed and analyzed bulk RNA-seq data and performed GWCoGAPS and ProjectR analyses. S.M. and C.C. analyzed single cell RNA-seq data and performed ProjectR analyses. N.M., SK.K., S.S., D.J.H. performed immuno-fluorescence, microscopy acquisition and high-content image analysis. N.M., C.C., G.SO, D.J.H. performed lineage analysis. N.M. and K.R.M. performed neuro-morphology analysis. B.G.R. performed immuno-histochemistry and microscope acquisition of the monkey tissue slides. J.A. banked and organized monkey tissue. N.M., SK.K., G.SO., J.G.C., C.C., D.J.H. developed biological and bio-informatic pipelines to manipulate and analyze hPSCs. N.M., SK.K., G.S.O., D.J.H., C.C., N.S., P.R., R.D.M. interpreted the data. A.J.C., R.B., N.J.B., D.R.W., N.S., P.R. and R.D.M. directed the research. N.M., C.C., SK.K., R.D.M. wrote the manuscript. All authors participated in discussion of results and manuscript editing.

ACKNOWLEDGEMENTS

This work was supported by the Lieber Institute for Brain Development (LIBD) and the National Institutes of Health grants DA02399 and EY002593 to P.R. and MH106934, MH106874, MH116488, MH110926 and MH109904 to N.S.. E.J.F. and G.S.O. were also supported by the National Institutes of Health (CA177669, CA212007, CA006973), the Johns Hopkins University Discovery Award, and the Johns Hopkins University School of Medicine Synergy Award. We thank many members of LIBD and Yale Department of Neuroscience (Rakic and Sestan labs) for their helpful comments on this work and manuscript. We thank Dr. Alvaro Duque and MacBrainResource (https://medicine.yale.edu/neuroscience/macbrain/) for providing non-human pimate tissue for immunohistochemistry (NIMH R01-MH113257 to Dr. A Duque).

DECLARATION OF INTERESTS

The authors declare no competing interests.

FIGURE LEGENDS

Figure 1. Mouse cortical neurogenesis *in vitro* regulated by early FGF2 (**A**) Experimental design. NSCs were expanded in 10 ng/ml FGF2 (PS1) and re-plated (PS2) over rat astrocytes, or without astrocytes, as indicated for individual experiments. At passage, cells were exposed for 2 days to 0.1, 1 or 10 ng/ml FGF2 and then differentiated by FGF2 withdrawal and Neurotrophins addition. The derived cortical neurons were assessed several days later. F2: FGF2; NB: NeuroBasal medium. (**B**) Mean number of TuJ1$^+$ neurons/field, from 4 independent DIV 15 cultures. ANOVA comparing FGF2 doses ($p<0.05$). *: 0.1 vs 10. #: 1 vs 10. +: 0.1 vs 1. (**C**) Percentage of TuJ1$^+$ neurons expressing TLE4 (deep layers) or CUX1 (upper layers). ANOVA comparing FGF2 doses ($p<0.05$). *: 0.1 vs 10. #: 1 vs 10. +: 0.1 vs 1. **(D)** Mean frequency of EPSCs in DIV 15 neurons. t-test. (**E**) 6 of 11 GWCoGAPS patterns shown in Figure S2. Inset p-values indicate enrichment of genes annotated by gene ontology (GO) categories in each pattern.

Figure 2. Endogenous BMP signaling dynamics across *in vitro* neurogenesis (**A-C**) (Top) Expression of selected clusters of genes annotated by “BMP receptor signaling” from NCI (full dendrogram in Figure S4), correlating with (A) BMP7, (B) BMP4 and (C) BMP6. BMP7 was rapidly repressed in cells exposed to low FGF2 doses, BMP4 levels increased at the initiation of differentiation and BMP6 was expressed at late time points. (Bottom) Genes weight for each GWCoGAPS pattern. Color keys as in A. (**D**) Expression of BMP7, BMP4 and BMP6 from RNA-seq data. (**E**) (Left) Immuno-fluorescence images of pSMAD1/5. (Right) Mean signal intensity of pSMAD1/5 within individually nuclear segmented cells, ± St.Dev. ANOVA comparing FGF2 doses ($p<0.05$). *: 0.1 vs 10. #: 1 vs 10. +: 0.1 vs 1. (**F**) Proportion of pSMAD1/5$^+$ cells relative to total cells at DIV 2 at different FGF2 doses, without or with LDN193189. Mean values + St.Dev. (**G**) (Left) Immuno-fluorescence images of Synapsin1 in neurons cultured over rat astrocytes, at

different FGF2 doses without or with LDN193189. (Right) Synapsin1(SYN1) and Homer (HOM) punta counts per 100 µm of neurite length. Mean + St.Dev., t-test n > 5 fields per measurement.

Figure 3. Mouse NSC subtypes with selective FGF2-induced BMP signaling activation and distinct fate bias (**A**) Density plot of PDGFRα and EGFR expression in individual cells, 2 days after plating (from the experiment shown in Figure S5A). Color key: percentile cell counts per bin. (**B**) (Top) Immuno-fluorescence images of pSMAD1/5 in $EGFR_{high}$ and $PDGFR\alpha_{high}$ cells. Arrows show pSMAD1/5 signals in cells. (Bottom) Mean signal intensity of pSMAD1/5 and BMPR1A in individually segmented $EGFR_{high}$ and $PDGFR\alpha_{high}$ cells at DIV 2, ± St.Dev. t-test. (**C**) Lineage analysis of NSCs to derivative differentiated cells (related to Video S1-3). Commitment event plots across cell divisions (generations) from $PDGFR\alpha_{high}$ (top) or $EGFR_{high}$ cells (bottom) (see Methods for details). Ol, oligodendrocyte; As, astrocyte; Ne, neuron; D, death (apoptotic). *n*= total commitment events. (**D**) Raw fluorescence intensity of each marker in individual AAV5-GFP or AAV6-GFP- $TuJ1^+$ neurons at DIV 15. Mean values (lines). t-test.

Figure 4. Cortical neuron bias at a specific passage of human NSCs

(**A**) Representation of hNSC culture and cortical neuron differentiation. hNSCs were expanded in 20 ng/ml FGF2 at every passage from PS2. FGF2 modulation was applied only at terminal passage. Further neuron differentiation was induced at PS4, 6 days after exposing hNSCs to different doses of FGF2, by FGF2 withdrawal and Neurotrophins addition, as described in Figure 1. LSB: LDN193189 + SB431542 (See Methods); NB: NeuroBasal medium. (**B**) (i) GWCoGAPS patterns p5 and p22. (ii) Projections of macaque cortex data from (Bakken et al., 2016) into p5 and p22. CP: cortical plate; Hem: cortical hem; SVZ: subventricular zone; VZ: ventricular zone. (iii) t-distributed stochastic neighbor embedding (tSNE) plots showing projections of macaque E78 DLPFC single cell RNA-seq data set into p5 and p22 colored by magnitude of projection (**C**) (i) Immuno-fluorescence images of EGFR and TuJ1 co-stained cells, or pSMAD1/5. (ii) Mean fluorescence intensity in individual segmented cells for the indicated markers. (**D**) Percentage of the total HuC/HuD^+ neurons expressing the layer specific marker indicated (see methods), 21

days after FGF2 withdrawal. t-test**.** Representative immuno-fluorescence images are shown in Figure S8 (**E**) (Left) Mean frequency of spontaneous EPSCs recorded in neurons cultured over astrocytes, 17 days after FGF2 withdrawal (p=0.0031). (Right) Proportion of neurons with (blue) or without (red) firing action potentials. n= number of neurons recorded. **(F)** EGFR-BMP signaling interaction in RGCs of developing non-human primate cortex. Immuno-staining of E70 rhesus macaque dorsal parietal cortex tissues sections for EGFR (red; all panels) together with PAX6 (i), pSMAD1/5 (ii), pSMAD1/5 and NEUROD1 (iii is a higher magnification of (ii)), TBR2 (iv), TBR1 (v). Nuclei were stained with DAPI. In (i) arrows highlight $EGFR^+$ radially migrating early neurogenic cells (higher magnification shown in inset); in (ii) arrows highlight $EGFR^+$ RGCs expressing pSMAD1/5. (**G)** Neuronal transition states of RGCs in developing human cortex. (i-iv) tSNE plots of human fetal telencephalic single-cell RNA-seq data of 3495 cells from (Nowakowski et al., 2017). Depiction of cell classes and ages of the individual donors from which the cells derive is shown in Figure S9. (i) S-phase scores of individual cells calculated using Seurat in Bioconductor/R. Notice two populations of IPCs, one cycling (green circle) and a second that has exited the cell cycle (blue circle). (ii) SOX2 expression is high in a greater proportion of proliferating IPCs. (iii) EGFR expression is high in a greater proportion of proliferating IPCs. (iv) EOMES/TBR2 expression is high across both of these IPC populations. Other cell populations showing high EGFR expression include truncated (t)RGs and astrocytes (Astr) at later developmental stages (Figure S9), as indicated by labels and arrows.

Figure 5. Cortical organizer identities of human NSCs and progression to neuronal fates (**A**) (i) GWCoGAPS patterns p8, p11 and p2 are shown. (ii) Projections of macaque cortex data from (Bakken et al., 2016) into p8, p11 and p2. (**B**) Cortical hem related gene expression across passages and FGF2 doses. Gene list derived from data in panel (Aii) contrasting cortical hem with other developing cortical regions (see Methods for details). (**C**) Immuno-fluorescence images of (i) LMX1A and LHX2 co-immunostaining, (ii) FOXG1, (iii) EGFR and OTX2 co-immunostaining, at PS2-PS4 hNSCs in 0.1 ng/ml FGF2, 6 days after passage. FOXG1 (ii) and EGFR/OTX2 (iii) images are from the same field; (iv) Proportion of individual segmented cells for the indicated

markers; (v) Scatter plot of EGFR vs OTX2 expressing cells, colored by FOXG1 level. **(D)** Model of the hNSC state progression from PS2 to PS4. The markers shown in Figures 4, 5 and S7, S8 are indicated for discreate cell states. Lineage divergence of NSC towards hem-like or cortex-like identity is indicated by arrows.

REFERENCES

Adepoju, A., Micali, N., Ogawa, K., Hoeppner, D.J., and McKay, R.D. (2014). FGF2 and insulin signaling converge to regulate cyclin D expression in multipotent neural stem cells. Stem Cells *32*, 770-778.

Amiri, A., Coppola, G., Scuderi, S., Wu, F., Roychowdhury, T., Liu, F., Pochareddy, S., Shin, Y., Safi, A., Song, L.*, et al.* (2018). Transcriptome and epigenome landscape of human cortical development modeled in organoids. Science *362*.

Androutsellis-Theotokis, A., Leker, R.R., Soldner, F., Hoeppner, D.J., Ravin, R., Poser, S.W., Rueger, M.A., Bae, S.K., Kittappa, R., and McKay, R.D. (2006). Notch signalling regulates stem cell numbers in vitro and in vivo. Nature *442*, 823-826.

Androutsellis-Theotokis, A., Murase, S., Boyd, J.D., Park, D.M., Hoeppner, D.J., Ravin, R., and McKay, R.D. (2008). Generating neurons from stem cells. Methods Mol Biol *438*, 31-38.

Angevine, J.B., Jr., and Sidman, R.L. (1961). Autoradiographic study of cell migration during histogenesis of cerebral cortex in the mouse. Nature *192*, 766-768.

Armentano, M., Chou, S.J., Tomassy, G.S., Leingartner, A., O'Leary, D.D., and Studer, M. (2007). COUP-TFI regulates the balance of cortical patterning between frontal/motor and sensory areas. Nat Neurosci *10*, 1277-1286.

Arnold, S.J., Huang, G.J., Cheung, A.F., Era, T., Nishikawa, S., Bikoff, E.K., Molnar, Z., Robertson, E.J., and Groszer, M. (2008). The T-box transcription factor Eomes/Tbr2 regulates neurogenesis in the cortical subventricular zone. Genes Dev *22*, 2479-2484.

Bakken, T.E., Miller, J.A., Ding, S.L., Sunkin, S.M., Smith, K.A., Ng, L., Szafer, A., Dalley, R.A., Royall, J.J., Lemon, T.*, et al.* (2016). A comprehensive transcriptional map of primate brain development. Nature *535*, 367-375.

Bishop, K.M., Goudreau, G., and O'Leary, D.D. (2000). Regulation of area identity in the mammalian neocortex by Emx2 and Pax6. Science *288*, 344-349.

Brennand, K., Savas, J.N., Kim, Y., Tran, N., Simone, A., Hashimoto-Torii, K., Beaumont, K.G., Kim, H.J., Topol, A., Ladran, I.*, et al.* (2015). Phenotypic differences in hiPSC NPCs derived from patients with schizophrenia. Mol Psychiatry *20*, 361-368.

Bulchand, S., Grove, E.A., Porter, F.D., and Tole, S. (2001). LIM-homeodomain gene Lhx2 regulates the formation of the cortical hem. Mech Dev *100*, 165-175.

Burrows, R.C., Wancio, D., Levitt, P., and Lillien, L. (1997). Response diversity and the timing of progenitor cell maturation are regulated by developmental changes in EGFR expression in the cortex. Neuron *19*, 251-267.

Butler, A., Hoffman, P., Smibert, P., Papalexi, E., and Satija, R. (2018). Integrating single-cell transcriptomic data across different conditions, technologies, and species. Nat Biotechnol *36*, 411-420.

Bystron, I., Blakemore, C., and Rakic, P. (2008). Development of the human cerebral cortex: Boulder Committee revisited. Nat Rev Neurosci *9*, 110-122.

Caronia-Brown, G., Yoshida, M., Gulden, F., Assimacopoulos, S., and Grove, E.A. (2014). The cortical hem regulates the size and patterning of neocortex. Development *141*, 2855-2865.

Cattaneo, E., and McKay, R. (1990). Proliferation and differentiation of neuronal stem cells regulated by nerve growth factor. Nature *347*, 762-765.

Chambers, S.M., Fasano, C.A., Papapetrou, E.P., Tomishima, M., Sadelain, M., and Studer, L. (2009). Highly efficient neural conversion of human ES and iPS cells by dual inhibition of SMAD signaling. Nat Biotechnol *27*, 275-280.

Chen, K.G., Mallon, B.S., Hamilton, R.S., Kozhich, O.A., Park, K., Hoeppner, D.J., Robey, P.G., and McKay, R.D. (2012). Non-colony type monolayer culture of human embryonic stem cells. Stem cell research *9*, 237-248.

Chizhikov, V.V., Lindgren, A.G., Mishima, Y., Roberts, R.W., Aldinger, K.A., Miesegaes, G.R., Currle, D.S., Monuki, E.S., and Millen, K.J. (2010). Lmx1a regulates fates and location of cells originating from the cerebellar rhombic lip and telencephalic cortical hem. Proc Natl Acad Sci U S A *107*, 10725-10730.

Cholfin, J.A., and Rubenstein, J.L. (2007). Patterning of frontal cortex subdivisions by Fgf17. Proc Natl Acad Sci U S A *104*, 7652-7657.

Consortium, H.D.i. (2017). Developmental alterations in Huntington's disease neural cells and pharmacological rescue in cells and mice. Nat Neurosci *20*, 648-660.

Crawley, J.N., Heyer, W.D., and LaSalle, J.M. (2016). Autism and Cancer Share Risk Genes, Pathways, and Drug Targets. Trends Genet *32*, 139-146.

de la Torre-Ubieta, L., Stein, J.L., Won, H., Opland, C.K., Liang, D., Lu, D., and Geschwind, D.H. (2018). The Dynamic Landscape of Open Chromatin during Human Cortical Neurogenesis. Cell *172*, 289-304 e218.

Di Pasquale, G., Davidson, B.L., Stein, C.S., Martins, I., Scudiero, D., Monks, A., and Chiorini, J.A. (2003). Identification of PDGFR as a receptor for AAV-5 transduction. Nat Med *9*, 1306-1312.

Edri, R., Yaffe, Y., Ziller, M.J., Mutukula, N., Volkman, R., David, E., Jacob-Hirsch, J., Malcov, H., Levy, C., Rechavi, G.*, et al.* (2015). Analysing human neural stem cell ontogeny by consecutive isolation of Notch active neural progenitors. Nat Commun *6*, 6500.

Englund, C., Fink, A., Lau, C., Pham, D., Daza, R.A., Bulfone, A., Kowalczyk, T., and Hevner, R.F. (2005). Pax6, Tbr2, and Tbr1 are expressed sequentially by radial glia, intermediate progenitor cells, and postmitotic neurons in developing neocortex. J Neurosci *25*, 247-251.

Ernst, C. (2016). Proliferation and Differentiation Deficits are a Major Convergence Point for Neurodevelopmental Disorders. Trends Neurosci *39*, 290-299.

Fertig, E.J., Ding, J., Favorov, A.V., Parmigiani, G., and Ochs, M.F. (2010). CoGAPS: an R/C++ package to identify patterns and biological process activity in transcriptomic data. Bioinformatics *26*, 2792-2793.

Fertig, E.J., Ren, Q., Cheng, H., Hatakeyama, H., Dicker, A.P., Rodeck, U., Considine, M., Ochs, M.F., and Chung, C.H. (2012). Gene expression signatures modulated by epidermal growth factor receptor activation and their relationship to cetuximab resistance in head and neck squamous cell carcinoma. BMC Genomics *13*, 160.

Fertig, E.J., Stein-O'Brien, G., Jaffe, A., and Colantuoni, C. (2014). Pattern identification in time-course gene expression data with the CoGAPS matrix factorization. Methods Mol Biol *1101*, 87-112.

Fujimori, K., Ishikawa, M., Otomo, A., Atsuta, N., Nakamura, R., Akiyama, T., Hadano, S., Aoki, M., Saya, H., Sobue, G.*, et al.* (2018). Modeling sporadic ALS in iPSC-derived motor neurons identifies a potential therapeutic agent. Nat Med *24*, 1579-1589.

Fukuchi-Shimogori, T., and Grove, E.A. (2001). Neocortex patterning by the secreted signaling molecule FGF8. Science *294*, 1071-1074.

Geschwind, D.H., and Rakic, P. (2013). Cortical evolution: judge the brain by its cover. Neuron *80*, 633-647.

Grove, E.A., and Fukuchi-Shimogori, T. (2003). Generating the cerebral cortical area map. Annu Rev Neurosci *26*, 355-380.

Grove, E.A., Tole, S., Limon, J., Yip, L., and Ragsdale, C.W. (1998). The hem of the embryonic cerebral cortex is defined by the expression of multiple Wnt genes and is compromised in Gli3-deficient mice. Development *125*, 2315-2325.

Gulsuner, S., Walsh, T., Watts, A.C., Lee, M.K., Thornton, A.M., Casadei, S., Rippey, C., Shahin, H., Consortium on the Genetics of, S., Group, P.S.*, et al.* (2013). Spatial and temporal mapping of de novo mutations in schizophrenia to a fetal prefrontal cortical network. Cell *154*, 518-529.

Hanashima, C., Fernandes, M., Hebert, J.M., and Fishell, G. (2007). The role of Foxg1 and dorsal midline signaling in the generation of Cajal-Retzius subtypes. J Neurosci *27*, 11103-11111.

Hansen, D.V., Lui, J.H., Parker, P.R., and Kriegstein, A.R. (2010). Neurogenic radial glia in the outer subventricular zone of human neocortex. Nature *464*, 554-561.

Hansen, N., Grunewald, B., Weishaupt, A., Colaco, M.N., Toyka, K.V., Sommer, C., and Geis, C. (2013). Human Stiff person syndrome IgG-containing high-titer anti-GAD65 autoantibodies induce motor dysfunction in rats. Exp Neurol *239*, 202-209.

Hubler, Z., Allimuthu, D., Bederman, I., Elitt, M.S., Madhavan, M., Allan, K.C., Shick, H.E., Garrison, E., M, T.K., Factor, D.C.*, et al.* (2018). Accumulation of 8,9-unsaturated sterols drives oligodendrocyte formation and remyelination. Nature *560*, 372-376.

Jackson, E.L., Garcia-Verdugo, J.M., Gil-Perotin, S., Roy, M., Quinones-Hinojosa, A., VandenBerg, S., and Alvarez-Buylla, A. (2006). PDGFR alpha-positive B cells are neural stem cells in the adult SVZ that form glioma-like growths in response to increased PDGF signaling. Neuron *51*, 187-199.

Jaffe, A.E., Straub, R.E., Shin, J.H., Tao, R., Gao, Y., Collado-Torres, L., Kam-Thong, T., Xi, H.S., Quan, J., Chen, Q.*, et al.* (2018). Developmental and genetic regulation of the human cortex transcriptome illuminate schizophrenia pathogenesis. Nat Neurosci *21*, 1117-1125.

Johe, K.K., Hazel, T.G., Muller, T., Dugich-Djordjevic, M.M., and McKay, R.D. (1996). Single factors direct the differentiation of stem cells from the fetal and adult central nervous system. Genes Dev *10*, 3129-3140.

Kim, J.H., Auerbach, J.M., Rodriguez-Gomez, J.A., Velasco, I., Gavin, D., Lumelsky, N., Lee, S.H., Nguyen, J., Sanchez-Pernaute, R., Bankiewicz, K.*, et al.* (2002). Dopamine neurons derived from embryonic stem cells function in an animal model of Parkinson's disease. Nature *418*, 50-56.

Kwan, K.Y., Lam, M.M., Johnson, M.B., Dube, U., Shim, S., Rasin, M.R., Sousa, A.M., Fertuzinhos, S., Chen, J.G., Arellano, J.I.*, et al.* (2012a). Species-dependent posttranscriptional regulation of NOS1 by FMRP in the developing cerebral cortex. Cell *149*, 899-911.

Kwan, K.Y., Sestan, N., and Anton, E.S. (2012b). Transcriptional co-regulation of neuronal migration and laminar identity in the neocortex. Development *139*, 1535-1546.

Lang, C., Campbell, K.R., Ryan, B.J., Carling, P., Attar, M., Vowles, J., Perestenko, O.V., Bowden, R., Baig, F., Kasten, M.*, et al.* (2018). Single-Cell Sequencing of iPSC-Dopamine Neurons Reconstructs Disease Progression and Identifies HDAC4 as a Regulator of Parkinson Cell Phenotypes. Cell Stem Cell.

Lehtinen, M.K., Zappaterra, M.W., Chen, X., Yang, Y.J., Hill, A.D., Lun, M., Maynard, T., Gonzalez, D., Kim, S., Ye, P.*, et al.* (2011). The cerebrospinal fluid provides a proliferative niche for neural progenitor cells. Neuron *69*, 893-905.

Lein, E.S., Belgard, T.G., Hawrylycz, M., and Molnar, Z. (2017). Transcriptomic Perspectives on Neocortical Structure, Development, Evolution, and Disease. Annu Rev Neurosci *40*, 629-652.

Li, M., Santpere, G., Imamura Kawasawa, Y., Evgrafov, O.V., Gulden, F.O., Pochareddy, S., Sunkin, S.M., Li, Z., Shin, Y., Zhu, Y.*, et al.* (2018). Integrative functional genomic analysis of human brain development and neuropsychiatric risks. Science *362*.

Li, W., Cogswell, C.A., and LoTurco, J.J. (1998). Neuronal differentiation of precursors in the neocortical ventricular zone is triggered by BMP. J Neurosci *18*, 8853-8862.

Lillien, L., and Raphael, H. (2000). BMP and FGF regulate the development of EGF-responsive neural progenitor cells. Development *127*, 4993-5005.

Mabie, P.C., Mehler, M.F., and Kessler, J.A. (1999). Multiple roles of bone morphogenetic protein signaling in the regulation of cortical cell number and phenotype. J Neurosci *19*, 7077-7088.

Madison, J.M., Zhou, F., Nigam, A., Hussain, A., Barker, D.D., Nehme, R., van der Ven, K., Hsu, J., Wolf, P., Fleishman, M.*, et al.* (2015). Characterization of bipolar disorder patient-specific induced pluripotent stem cells from a family reveals neurodevelopmental and mRNA expression abnormalities. Mol Psychiatry *20*, 703-717.

Mangale, V.S., Hirokawa, K.E., Satyaki, P.R., Gokulchandran, N., Chikbire, S., Subramanian, L., Shetty, A.S., Martynoga, B., Paul, J., Mai, M.V.*, et al.* (2008). Lhx2 selector activity specifies cortical identity and suppresses hippocampal organizer fate. Science *319*, 304-309.

Marchetto, M.C., Belinson, H., Tian, Y., Freitas, B.C., Fu, C., Vadodaria, K.C., Beltrao-Braga, P.C., Trujillo, C.A., Mendes, A.P., Padmanabhan, K.*, et al.* (2016). Altered proliferation and networks in neural cells derived from idiopathic autistic individuals. Mol Psychiatry.

Mariani, J., Coppola, G., Zhang, P., Abyzov, A., Provini, L., Tomasini, L., Amenduni, M., Szekely, A., Palejev, D., Wilson, M.*, et al.* (2015). FOXG1-Dependent Dysregulation of GABA/Glutamate Neuron Differentiation in Autism Spectrum Disorders. Cell *162*, 375-390.

Mariani, J., Simonini, M.V., Palejev, D., Tomasini, L., Coppola, G., Szekely, A.M., Horvath, T.L., and Vaccarino, F.M. (2012). Modeling human cortical development in vitro using induced pluripotent stem cells. Proc Natl Acad Sci U S A *109*, 12770-12775.

Mendoza, M.C., Er, E.E., and Blenis, J. (2011). The Ras-ERK and PI3K-mTOR pathways: cross-talk and compensation. Trends Biochem Sci *36*, 320-328.

Miyashita-Lin, E.M., Hevner, R., Wassarman, K.M., Martinez, S., and Rubenstein, J.L. (1999). Early neocortical regionalization in the absence of thalamic innervation. Science *285*, 906-909.

Mo, Z., and Zecevic, N. (2008). Is Pax6 critical for neurogenesis in the human fetal brain? Cereb Cortex *18*, 1455-1465.

Molyneaux, B.J., Arlotta, P., Menezes, J.R., and Macklis, J.D. (2007). Neuronal subtype specification in the cerebral cortex. Nat Rev Neurosci *8*, 427-437.

Monuki, E.S., Porter, F.D., and Walsh, C.A. (2001). Patterning of the dorsal telencephalon and cerebral cortex by a roof plate-Lhx2 pathway. Neuron *32*, 591-604.

Nakagawa, Y., Johnson, J.E., and O'Leary, D.D. (1999). Graded and areal expression patterns of regulatory genes and cadherins in embryonic neocortex independent of thalamocortical input. J Neurosci *19*, 10877-10885.

Namba, T., and Huttner, W.B. (2017). Neural progenitor cells and their role in the development and evolutionary expansion of the neocortex. Wiley Interdiscip Rev Dev Biol *6*.

Nowakowski, T.J., Bhaduri, A., Pollen, A.A., Alvarado, B., Mostajo-Radji, M.A., Di Lullo, E., Haeussler, M., Sandoval-Espinosa, C., Liu, S.J., Velmeshev, D.*, et al.* (2017). Spatiotemporal gene expression trajectories reveal developmental hierarchies of the human cortex. Science *358*, 1318-1323.

Nowakowski, T.J., Pollen, A.A., Sandoval-Espinosa, C., and Kriegstein, A.R. (2016). Transformation of the Radial Glia Scaffold Demarcates Two Stages of Human Cerebral Cortex Development. Neuron *91*, 1219-1227.

O'Leary, D.D., Chou, S.J., and Sahara, S. (2007). Area patterning of the mammalian cortex. Neuron *56*, 252-269.

Okabe, S., Forsberg-Nilsson, K., Spiro, A.C., Segal, M., and McKay, R.D. (1996). Development of neuronal precursor cells and functional postmitotic neurons from embryonic stem cells in vitro. Mech Dev *59*, 89-102.

Parikshak, N.N., Luo, R., Zhang, A., Won, H., Lowe, J.K., Chandran, V., Horvath, S., and Geschwind, D.H. (2013). Integrative functional genomic analyses implicate specific molecular pathways and circuits in autism. Cell *155*, 1008-1021.

Pollen, A.A., Nowakowski, T.J., Chen, J., Retallack, H., Sandoval-Espinosa, C., Nicholas, C.R., Shuga, J., Liu, S.J., Oldham, M.C., Diaz, A.*, et al.* (2015). Molecular identity of human outer radial glia during cortical development. Cell *163*, 55-67.

Qi, Y., Zhang, X.J., Renier, N., Wu, Z., Atkin, T., Sun, Z., Ozair, M.Z., Tchieu, J., Zimmer, B., Fattahi, F.*, et al.* (2017). Combined small-molecule inhibition accelerates the derivation of functional cortical neurons from human pluripotent stem cells. Nat Biotechnol *35*, 154-163.

Rakic, P. (1974). Neurons in rhesus monkey visual cortex: systematic relation between time of origin and eventual disposition. Science *183*, 425-427.

Rakic, P. (1988). Specification of cerebral cortical areas. Science *241*, 170-176.

Rash, B.G., and Grove, E.A. (2006). Area and layer patterning in the developing cerebral cortex. Curr Opin Neurobiol *16*, 25-34.

Rash, B.G., Lim, H.D., Breunig, J.J., and Vaccarino, F.M. (2011). FGF signaling expands embryonic cortical surface area by regulating Notch-dependent neurogenesis. J Neurosci *31*, 15604-15617.

Ravin, R., Hoeppner, D.J., Munno, D.M., Carmel, L., Sullivan, J., Levitt, D.L., Miller, J.L., Athaide, C., Panchision, D.M., and McKay, R.D. (2008). Potency and fate specification in CNS stem cell populations in vitro. Cell Stem Cell *3*, 670-680.

Renner, M., Lancaster, M.A., Bian, S., Choi, H., Ku, T., Peer, A., Chung, K., and Knoblich, J.A. (2017). Self-organized developmental patterning and differentiation in cerebral organoids. EMBO J *36*, 1316-1329.

Sakaguchi, H., Kadoshima, T., Soen, M., Narii, N., Ishida, Y., Ohgushi, M., Takahashi, J., Eiraku, M., and Sasai, Y. (2015). Generation of functional hippocampal neurons from self-organizing human embryonic stem cell-derived dorsomedial telencephalic tissue. Nat Commun *6*, 8896.

Sandberg, M., Flandin, P., Silberberg, S., Su-Feher, L., Price, J.D., Hu, J.S., Kim, C., Visel, A., Nord, A.S., and Rubenstein, J.L. (2016). Transcriptional Networks Controlled by NKX2-1 in the Development of Forebrain GABAergic Neurons. Neuron *91*, 1260-1275.

Saxena, M., Agnihotri, N., and Sen, J. (2018). Perturbation of canonical and non-canonical BMP signaling affects migration, polarity and dendritogenesis of mouse cortical neurons. Development *145*.

Shen, Q., Wang, Y., Dimos, J.T., Fasano, C.A., Phoenix, T.N., Lemischka, I.R., Ivanova, N.B., Stifani, S., Morrisey, E.E., and Temple, S. (2006). The timing of cortical neurogenesis is encoded within lineages of individual progenitor cells. Nat Neurosci *9*, 743-751.

Shi, Y., Kirwan, P., Smith, J., Robinson, H.P., and Livesey, F.J. (2012). Human cerebral cortex development from pluripotent stem cells to functional excitatory synapses. Nat Neurosci *15*, 477-486, S471.

Shimogori, T., and Grove, E.A. (2005). Fibroblast growth factor 8 regulates neocortical guidance of area-specific thalamic innervation. J Neurosci *25*, 6550-6560.

State, M.W., and Sestan, N. (2012). Neuroscience. The emerging biology of autism spectrum disorders. Science *337*, 1301-1303.

Stein-O'Brien, G.L., Carey, J.L., Lee, W.S., Considine, M., Favorov, A.V., Flam, E., Guo, T., Li, S., Marchionni, L., Sherman, T.*, et al.* (2017). PatternMarkers & GWCoGAPS for novel data-driven biomarkers via whole transcriptome NMF. Bioinformatics.

Sun, Y., Goderie, S.K., and Temple, S. (2005). Asymmetric distribution of EGFR receptor during mitosis generates diverse CNS progenitor cells. Neuron *45*, 873-886.

Sur, M., and Rubenstein, J.L. (2005). Patterning and plasticity of the cerebral cortex. Science *310*, 805-810.

Tiberi, L., Vanderhaeghen, P., and van den Ameele, J. (2012). Cortical neurogenesis and morphogens: diversity of cues, sources and functions. Curr Opin Cell Biol *24*, 269-276.

Vaccarino, F.M., Schwartz, M.L., Raballo, R., Nilsen, J., Rhee, J., Zhou, M., Doetschman, T., Coffin, J.D., Wyland, J.J., and Hung, Y.T. (1999). Changes in cerebral cortex size are governed by fibroblast growth factor during embryogenesis. Nat Neurosci *2*, 848.

van Dijk, D., Sharma, R., Nainys, J., Yim, K., Kathail, P., Carr, A.J., Burdziak, C., Moon, K.R., Chaffer, C.L., Pattabiraman, D.*, et al.* (2018). Recovering Gene Interactions from Single-Cell Data Using Data Diffusion. Cell.

Wamsley, B., and Fishell, G. (2017). Genetic and activity-dependent mechanisms underlying interneuron diversity. Nat Rev Neurosci *18*, 299-309.

Wang, D., Liu, S., Warrell, J., Won, H., Shi, X., Navarro, F.C.P., Clarke, D., Gu, M., Emani, P., Yang, Y.T.*, et al.* (2018). Comprehensive functional genomic resource and integrative model for the human brain. Science *362*.

Weller, M.L., Amornphimoltham, P., Schmidt, M., Wilson, P.A., Gutkind, J.S., and Chiorini, J.A. (2010). Epidermal growth factor receptor is a co-receptor for adeno-associated virus serotype 6. Nat Med *16*, 662-664.

Willsey, A.J., Sanders, S.J., Li, M., Dong, S., Tebbenkamp, A.T., Muhle, R.A., Reilly, S.K., Lin, L., Fertuzinhos, S., Miller, J.A.*, et al.* (2013). Coexpression networks implicate human midfetal deep cortical projection neurons in the pathogenesis of autism. Cell *155*, 997-1007.

Wonders, C.P., and Anderson, S.A. (2006). The origin and specification of cortical interneurons. Nat Rev Neurosci *7*, 687-696.

Xu, X., Wells, A.B., O'Brien, D.R., Nehorai, A., and Dougherty, J.D. (2014). Cell type-specific expression analysis to identify putative cellular mechanisms for neurogenetic disorders. J Neurosci *34*, 1420-1431.

Zerbino, D.R., Achuthan, P., Akanni, W., Amode, M.R., Barrell, D., Bhai, J., Billis, K., Cummins, C., Gall, A., Giron, C.G.*, et al.* (2018). Ensembl 2018. Nucleic Acids Res *46*, D754-D761.

Zhu, Y., Sousa, A.M.M., Gao, T., Skarica, M., Li, M., Santpere, G., Esteller-Cucala, P., Juan, D., Ferrandez-Peral, L., Gulden, F.O.*, et al.* (2018). Spatiotemporal transcriptomic divergence across human and macaque brain development. Science *362*.

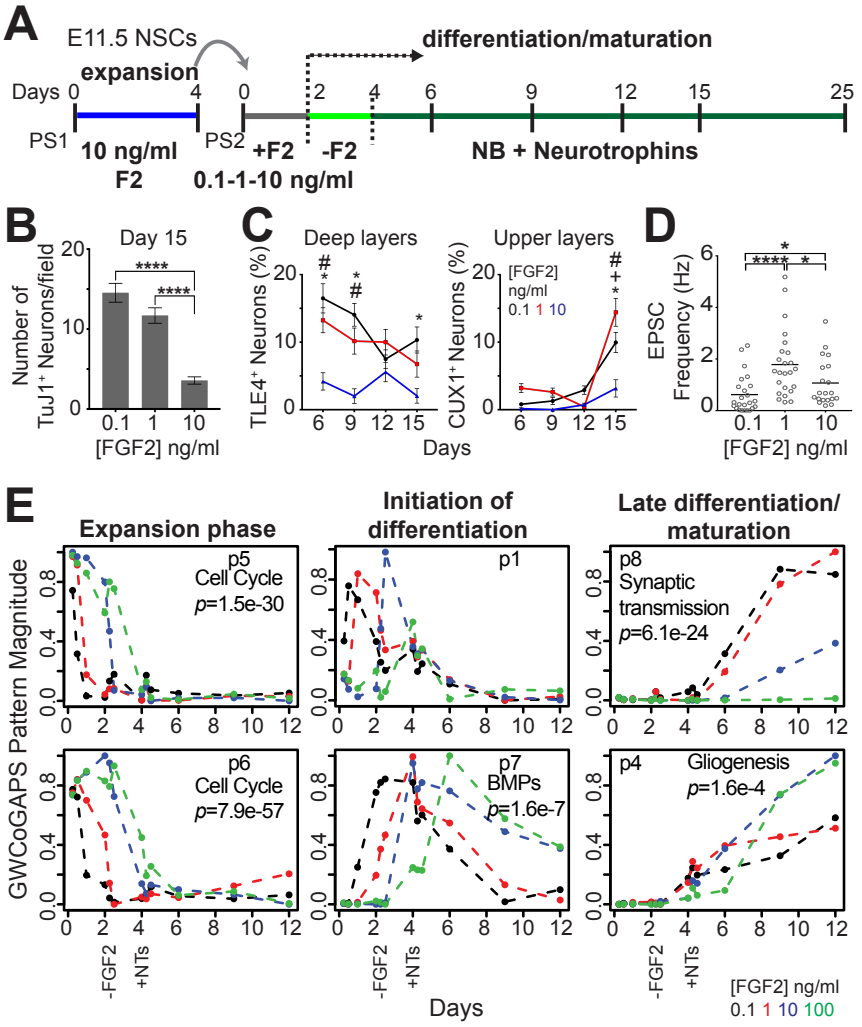
A
E11.5 NSCs
expansion
differentiation/maturation
Days 0
4
0
2
4
6
9
12
15
25
PS1
PS2
10 ng/ml
F2
+F2
-F2
0.1-1-10 ng/ml
NB + Neurotrophins
B
Day 15
Number of
TuJ1+ Neurons/field
****
****
[FGF2] ng/ml
C
Deep layers
Upper layers
TLE4+ Neurons (%)
CUX1+ Neurons (%)
[FGF2]
ng/ml
0.1 1 10
Days
D
EPSC
Frequency (Hz)
[FGF2] ng/ml
E
Expansion phase
Initiation of
differentiation
Late differentiation/
maturation
GWCoGAPS Pattern Magnitude
p5
Cell Cycle
p=1.5e-30
p1
p8
Synaptic
transmission
p=6.1e-24
p6
Cell Cycle
p=7.9e-57
p7
BMPs
p=1.6e-7
p4
Gliogenesis
p=1.6e-4
-FGF2
+NTs
Days
[FGF2] ng/ml
0.1 1 10 100

Figure 1

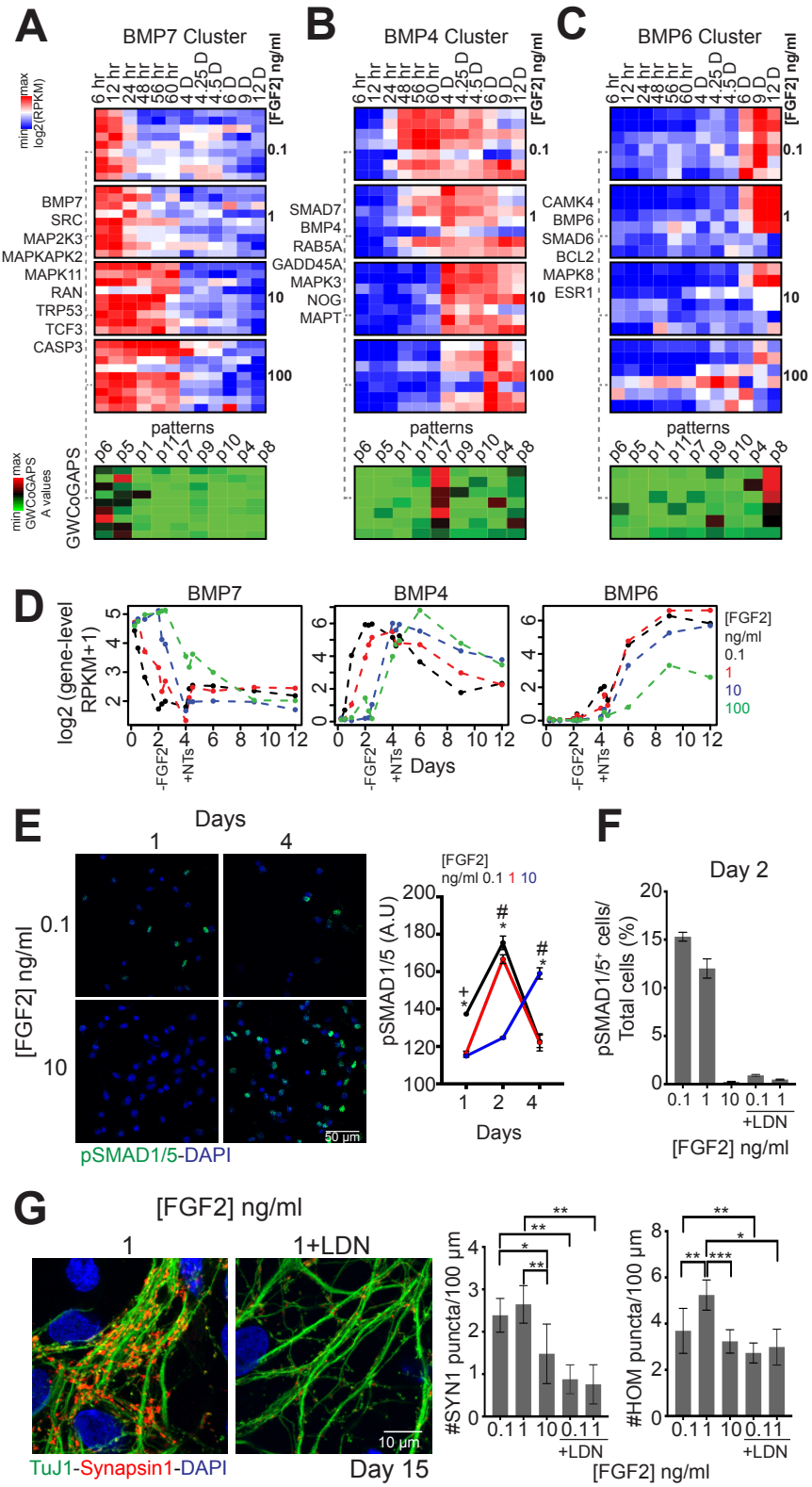
A
BMP7 Cluster
B
BMP4 Cluster
C
BMP6 Cluster
6 hr
12 hr
24 hr
48 hr
56 hr
60 hr
4 D
4.25 D
4.5 D
6 D
9 D
12 D
[FGF2] ng/ml
0.1
1
10
100
max
min
log2(RPKM)
BMP7
SRC
MAP2K3
MAPKAPK2
MAPK11
RAN
TRP53
TCF3
CASP3
SMAD7
BMP4
RAB5A
GADD45A
MAPK3
NOG
MAPT
CAMK4
BMP6
SMAD6
BCL2
MAPK8
ESR1
patterns
p6
p5
p1
p11
p7
p9
p10
p4
p8
GWCoGAPS
GWCoGAPS A values
D
BMP7
BMP4
BMP6
log2 (gene-level RPKM+1)
-FGF2
+NTs
Days
[FGF2] ng/ml
0.1
1
10
100
E
Days
1
4
[FGF2] ng/ml
0.1
10
50 µm
pSMAD1/5-DAPI
[FGF2] ng/ml 0.1 1 10
pSMAD1/5 (A.U)
Days
F
Day 2
pSMAD1/5+ cells/ Total cells (%)
+LDN
[FGF2] ng/ml
G
[FGF2] ng/ml
1
1+LDN
10 µm
TuJ1-Synapsin1-DAPI
Day 15
#SYN1 puncta/100 µm
#HOM puncta/100 µm
+LDN
[FGF2] ng/ml

Figure 2

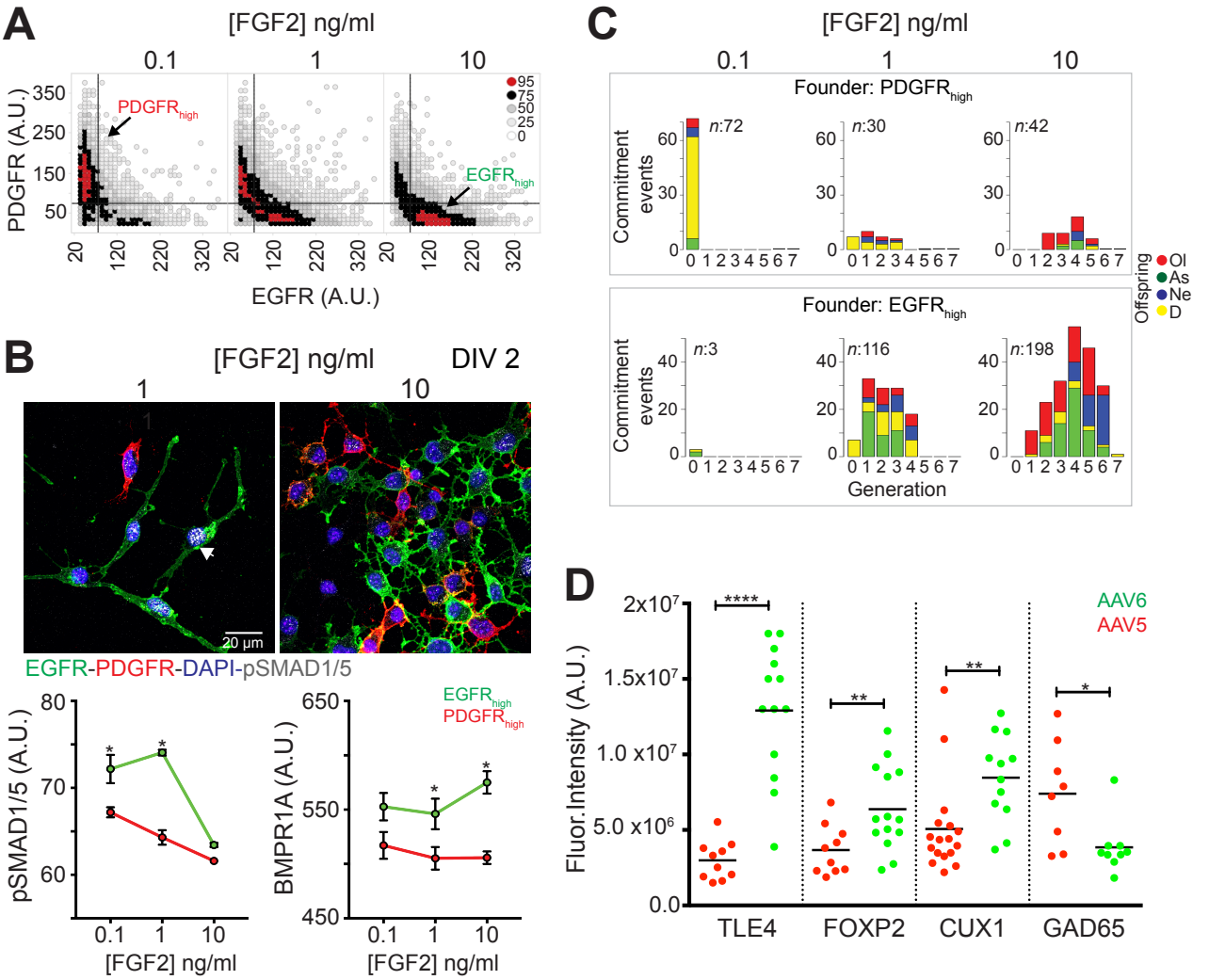
A
[FGF2] ng/ml
0.1
1
10
PDGFR (A.U.)
350
250
150
50
PDGFRhigh
EGFRhigh
95
75
50
25
0
20
120
220
320
EGFR (A.U.)
B
[FGF2] ng/ml
DIV 2
1
10
20 µm
EGFR-PDGFR-DAPI-pSMAD1/5
pSMAD1/5 (A.U.)
80
70
60
0.1
1
10
[FGF2] ng/ml
BMPR1A (A.U.)
650
550
450
EGFRhigh
PDGFRhigh
C
[FGF2] ng/ml
Founder: PDGFRhigh
Commitment events
n:72
n:30
n:42
Founder: EGFRhigh
n:3
n:116
n:198
Generation
Offspring
Ol
As
Ne
D
D
Fluor. Intensity (A.U.)
2x10⁷
1.5x10⁷
1.0 x10⁷
5.0 x10⁶
0.0
****
**
*
AAV6
AAV5
TLE4
FOXP2
CUX1
GAD65

Figure 3

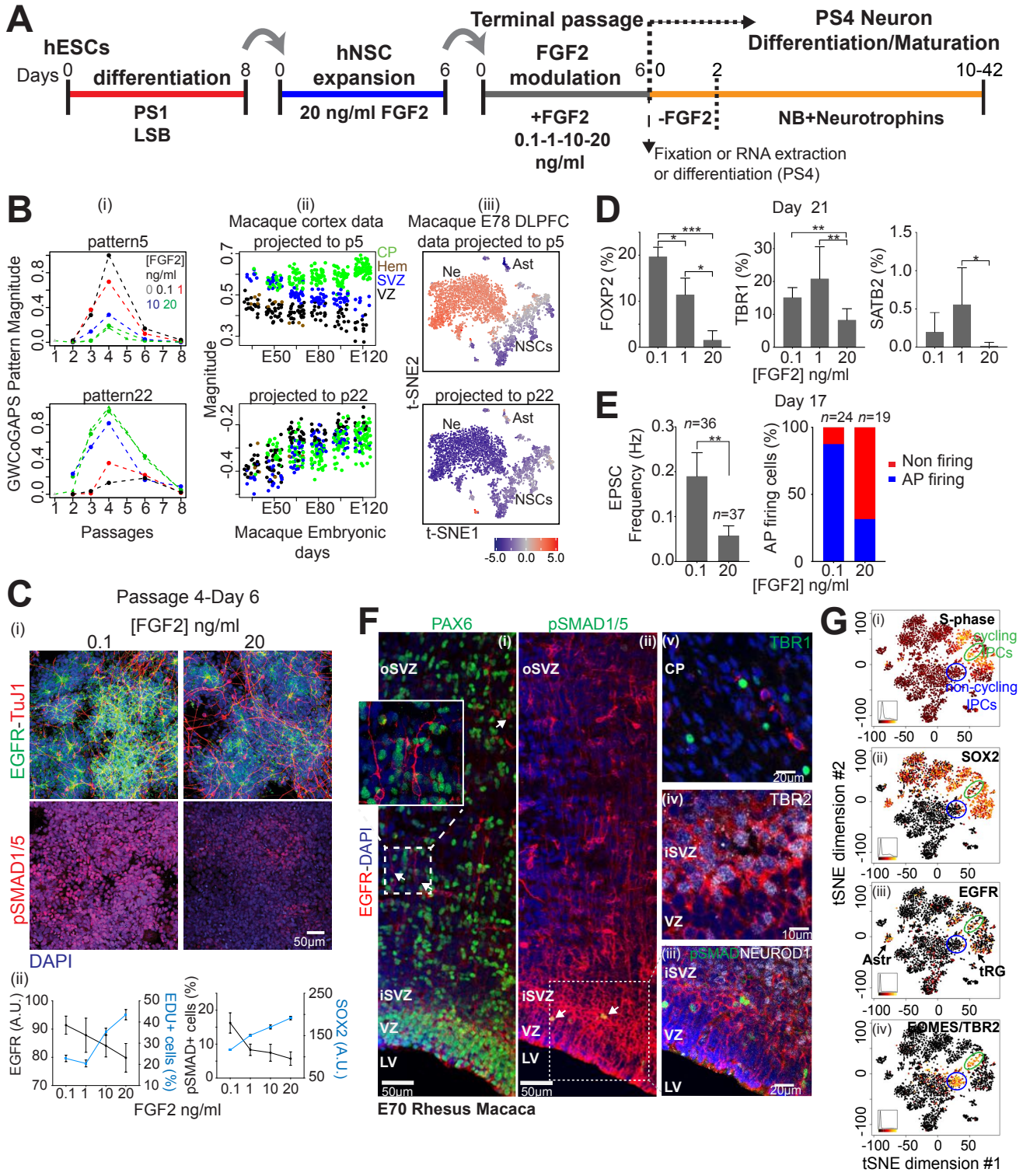
A
hESCs
Days 0
differentiation
8
PS1
LSB
0
hNSC
expansion
6
20 ng/ml FGF2
0
Terminal passage
FGF2
modulation
6
+FGF2
0.1-1-10-20
ng/ml
0
2
-FGF2
PS4 Neuron
Differentiation/Maturation
10-42
NB+Neurotrophins
Fixation or RNA extraction
or differentiation (PS4)
B
(i)
pattern5
[FGF2]
ng/ml
0 0.1 1
10 20
pattern22
GWCoGAPS Pattern Magnitude
Passages
(ii)
Macaque cortex data
projected to p5
CP
Hem
SVZ
VZ
projected to p22
Magnitude
E50 E80 E120
Macaque Embryonic
days
(iii)
Macaque E78 DLPFC
data projected to p5
Ne
Ast
NSCs
projected to p22
t-SNE2
t-SNE1
-5.0 0.0 5.0
D
Day 21
FOXP2 (%)
TBR1 (%)
SATB2 (%)
[FGF2] ng/ml
E
Day 17
EPSC
Frequency (Hz)
n=36
n=37
AP firing cells (%)
n=24 n=19
Non firing
AP firing
[FGF2] ng/ml
C
Passage 4-Day 6
(i)
[FGF2] ng/ml
0.1
20
EGFR-TuJ1
pSMAD1/5
DAPI
50µm
(ii)
EGFR (A.U.)
EDU+ cells (%)
pSMAD+ cells (%)
SOX2 (A.U.)
FGF2 ng/ml
F
PAX6
pSMAD1/5
(i)
(ii)
(v)
TBR1
CP
20µm
oSVZ
EGFR-DAPI
(iv)
TBR2
iSVZ
VZ
10µm
(iii)
pSMAD
NEUROD1
iSVZ
VZ
LV
50µm
20µm
E70 Rhesus Macaca
G
(i)
S-phase
cycling
IPCs
non-cycling
IPCs
(ii)
SOX2
(iii)
EGFR
Astr
tRG
(iv)
EOMES/TBR2
tSNE dimension #2
tSNE dimension #1

Figure 4

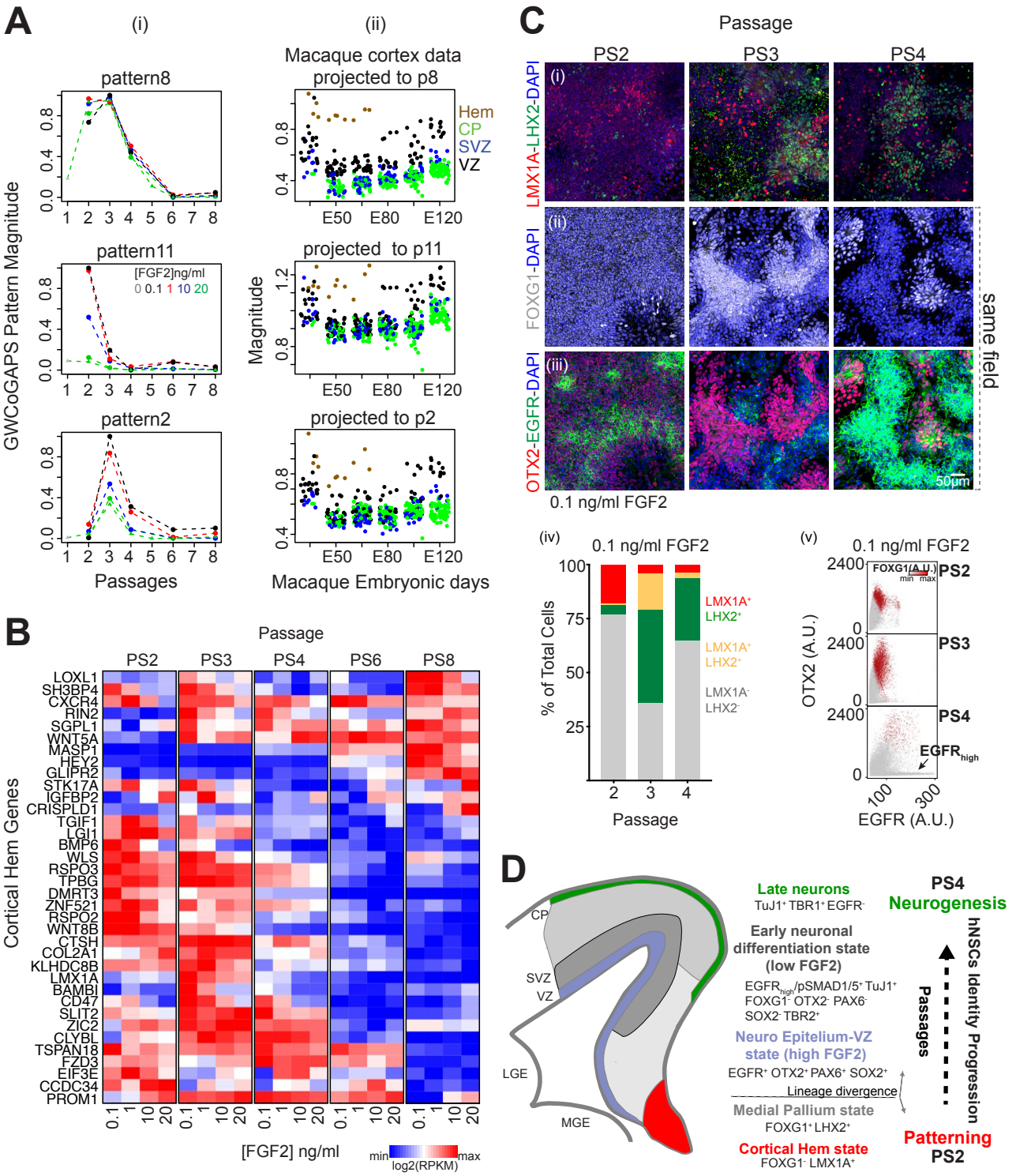
A
(i)
(ii)
Macaque cortex data projected to p8
pattern8
Hem
CP
SVZ
VZ
pattern11
[FGF2]ng/ml
0 0.1 1 10 20
projected to p11
Magnitude
pattern2
projected to p2
GWCoGAPS Pattern Magnitude
Passages
Macaque Embryonic days
B
Passage
PS2
PS3
PS4
PS6
PS8
Cortical Hem Genes
LOXL1
SH3BP4
CXCR4
RIN2
SGPL1
WNT5A
MASP1
HEY2
GLIPR2
STK17A
IGFBP2
CRISPLD1
TGIF1
LGI1
BMP6
WLS
RSPO3
TPBG
DMRT3
ZNF521
RSPO2
WNT8B
CTSH
COL2A1
KLHDC8B
LMX1A
BAMBI
CD47
SLIT2
ZIC2
CLYBL
TSPAN18
FZD3
EIF3E
CCDC34
PROM1
[FGF2] ng/ml
min
max
log2(RPKM)
C
Passage
PS2
PS3
PS4
LMX1A-LHX2-DAPI
FOXG1-DAPI
OTX2-EGFR-DAPI
same field
50µm
0.1 ng/ml FGF2
(iv)
0.1 ng/ml FGF2
% of Total Cells
LMX1A+ LHX2+
LMX1A+ LHX2+
LMX1A- LHX2-
Passage
(v)
0.1 ng/ml FGF2
FOXG1(A.U.)
min max
OTX2 (A.U.)
EGFRhigh
EGFR (A.U.)
D
CP
SVZ
VZ
LGE
MGE
Late neurons
TuJ1+ TBR1+ EGFR-
Early neuronal differentiation state (low FGF2)
EGFRhigh/pSMAD1/5+ TuJ1+
FOXG1- OTX2- PAX6-
SOX2- TBR2+
Neuro Epitelium-VZ state (high FGF2)
EGFR+ OTX2+ PAX6+ SOX2+
Lineage divergence
Medial Pallium state
FOXG1+ LHX2+
Cortical Hem state
FOXG1- LMX1A+
PS4
Neurogenesis
hNSCs Identity Progression
Passages
Patterning
PS2

Figure 5